

Control of the high-order harmonics cutoff through the combination of a chirped laser and static electric field

Yang Xiang,^{1,2} Yueping Niu,^{1,*} and Shangqing Gong^{1,†}

¹State Key Laboratory of High Field Laser Physics, Shanghai Institute of Optics and Fine Mechanics, Chinese Academy of Science, Shanghai 201800, China

²College of Computer Science and Technology, Henan Polytechnic University, Jiaozuo 454000, China

(Received 22 July 2008; revised manuscript received 7 April 2009; published 28 May 2009)

The high-order harmonic generation for a one-dimensional hydrogen atom model in the combination of the chirped laser pulse and static field is theoretically investigated. Here we explore a novel physical mechanism of the significant extension of high-order-harmonic generation cutoff based on three-step model. It is shown that due to the asymmetry of the combined field the cutoff is substantially extended. If appropriate parameters are chosen, the cutoff of high-order harmonic generation can reach I_p+42U_p . Furthermore, an ultrabroad supercontinuum spectrum can be generated. When the phases are properly compensated for, an isolated 10 as pulse can be obtained.

DOI: 10.1103/PhysRevA.79.053419

PACS number(s): 42.65.Ky

It is well known that high-order harmonics are generated when atoms or molecules are irradiated by intense laser field. In recent years, high-order harmonic generation (HHG) has become a very interesting topic of laser-atom interaction [1–3] because of a very important application of attosecond (as) pulse generation. Usually, there are two techniques to generate attosecond pulses [4]. One is to use few-cycle laser pulse, then the cutoff is continuous, and by spectrally selecting it a single attosecond pulse can be obtained [5]. The other is to use multicycle intense infrared pulse, then select many harmonics in the plateau, and an attosecond pulse train can be generated [6]. Many control ways have been studied in order to gain an isolated attosecond pulse [7–9]. In the presence of an intense static electric field, one can get a pulse of 220 as [10]. Using a chirped few-cycle laser field, a pulse of 108 as can be generated [11]. From the works mentioned above, one may want to know what would happen if the combination of chirped laser field and a static electric field is adopted in the HHG process. Based on this idea, we now investigate the HHG spectrum of atoms in this combined field.

We use one-dimensional time-dependent Schrödinger equation (TDSE) to describe the interaction between hydrogen atom and the combination of the chirped laser field and a static electric field in dipole approximations [atomic units (a.u.) are used in all equations in this paper unless otherwise mentioned]:

$$i \frac{\partial \psi(x,t)}{\partial t} = \left[-\frac{1}{2} \frac{\partial^2}{\partial x^2} + V(x) - xE(t) \right] \psi(x,t), \quad (1)$$

where the Coulomb potential $V(x)$ is represented by the “soft-core” potential which can be expressed as $V(x) = -1/\sqrt{1+x^2}$ [12]. The combined field is described as

$$E(t) = F\{f(t)\cos[\omega t + \delta(t)] - \alpha\}, \quad (2)$$

where F , $f(t)$, ω , and $\delta(t)$ are the amplitude, envelope, angular frequency, and time profile of the carrier envelope phase (CEP) of the laser field, respectively, and α is the ratio between the amplitude of the static and laser field. If $\alpha=0$ and $\delta(t)=0$, $E(t)$ is of symmetry. However the symmetry will be destroyed if $\alpha \neq 0$ or $\delta(t) \neq 0$. In all of our calculations, F is 0.12 a.u. (corresponds to intensity $I=5.0 \times 10^{14}$ W/cm²), ω is 0.057 a.u. (corresponds to wavelength $\lambda=800$ nm), and α is equal to 0.4 which is approximate to that in Ref. [10]. Although such a high static field can hardly be experimentally achieved nowadays, a low-frequency laser field (such as CO₂ laser field) can be used instead [13], which will be discussed later. The envelope of the laser field $f(t)$ has a type of Gaussian with 5 fs full width at half maximum (FWHM). The CEP considered in this paper is $\delta(t) = -\beta \tanh[(t-t_0)/\tau]$ [11]. The parameters β , t_0 , and τ are used to control the chirp form. Due to the recent advancement of comb laser technology, it is highly likely that such a time-varying CEP can be achieved in near future [11,14,15]. In our work, τ is chosen to be 200 a.u. Equation (1) can be integrated using split-operator method [12]. When the time-dependent wave

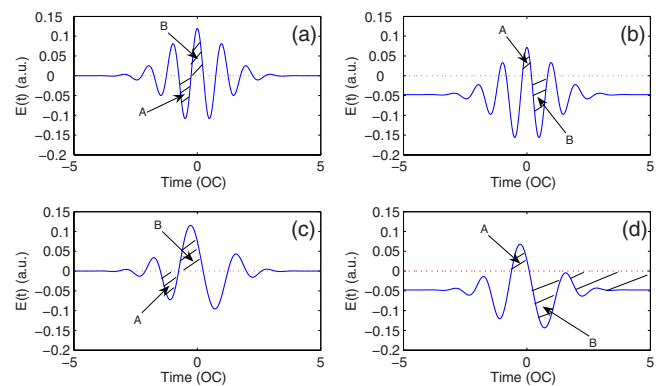


FIG. 1. (Color online) (a) Chirp-free laser field; (b) combination of chirp-free laser field and static electric field; (c) chirped laser field; (d) combination of chirped laser field and static electric field.

*niuyp@siom.ac.cn

†sqgong@siom.ac.cn

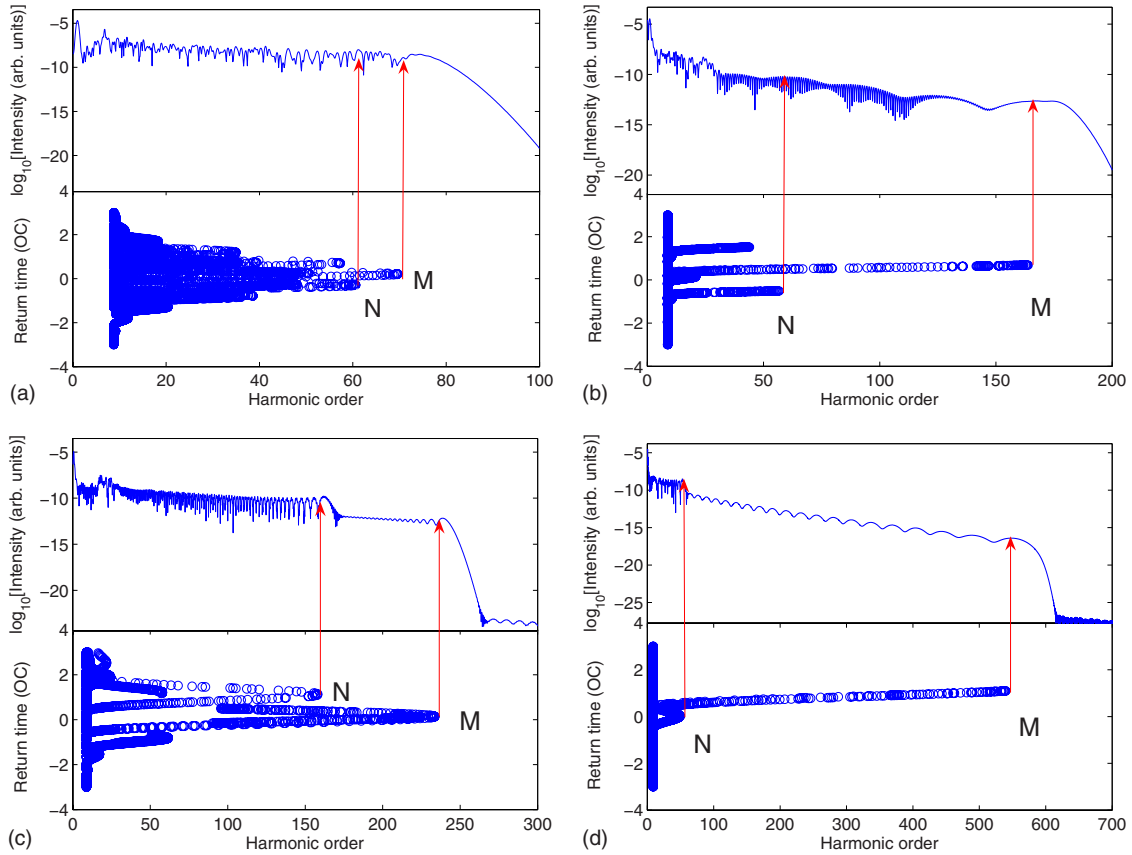


FIG. 2. (Color online) Comparison of the returning kinetic energy of the electron and HHG spectra in different field conditions: (a) chirp-free laser field; (b) combination of chirp-free laser and static electric field; (c) chirped laser field; (d) combination of chirped laser and static electric field. The parameters are same to those in Fig. 1.

function $\Psi(x, t)$ is obtained, we can then calculate the mean acceleration by means of Ehrenfest's theorem [16]:

$$d_A(t) \equiv \langle \ddot{x}(t) \rangle = - \langle \psi(x, t) | \frac{\partial V}{\partial x} - E(t) | \psi(x, t) \rangle. \quad (3)$$

The HHG spectrum then is obtained by taking the Fourier transform of $d_A(t)$.

In order to find how the combined field impacts on the HHG, we consider the HHG of hydrogen atom in four field cases: (a) chirp-free laser field, (b) combination of chirp-free laser field and static electric field, (c) chirped laser field, and (d) combination of chirped laser field and static electric field. The parameters β and t_0 for the chirped laser field in (c) and (d) are 6.25 and $\tau/7.0$. These fields are shown in Fig. 1.

The HHG spectra of the four cases are shown in Fig. 2. The cutoff of the spectra for (b), (c), and (d) is about 171st-, 238th-, and 551st-order harmonic, respectively, and each of them is much higher than the well-known value of $I_p + 3.17U_p$ [about 71th-order harmonic, just as shown in Fig. 2(a)], where I_p is the ionization potential $U_p [=F^2/(4\omega^2)]$ is the ponderomotive energy. To our surprise, the cutoff of HHG in (d) is much higher than that in (b) or (c). Furthermore, an ultrabroad supercontinuum spectrum which covers about 450 order harmonics appears in the case of combination of chirped laser field and static electric field.

Generally, the physical origin of the HHG from linearly polarized laser field can be qualitatively understood in the framework of semiclassical model which is called three-step-method (TSM) [17]: first, the electron tunnels through the barrier formed by the Coulomb potential and the laser field; next, it oscillates almost freely in the laser field; finally, it

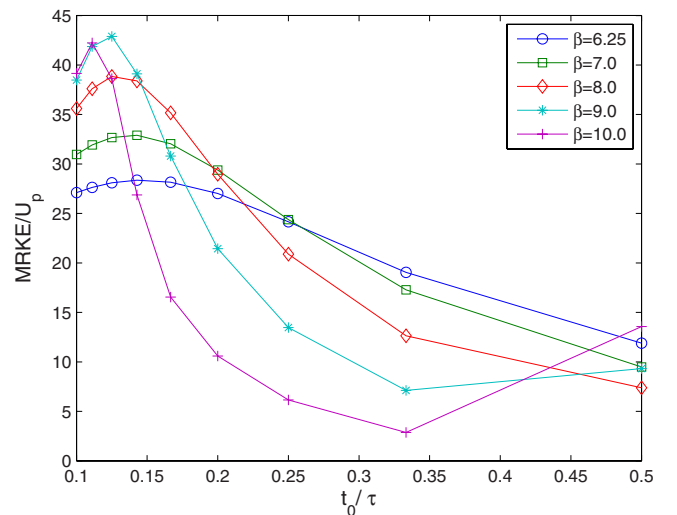


FIG. 3. (Color online) The maximum returning energy of electron as a function of β and t_0 .

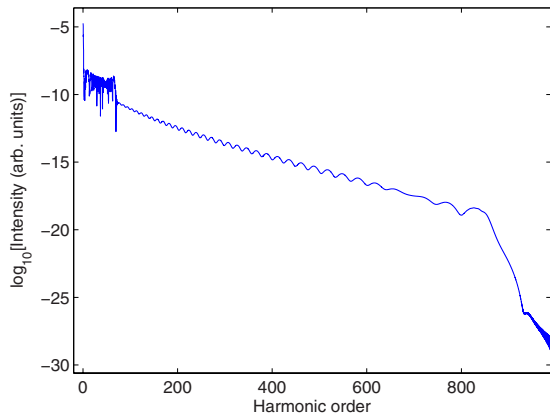


FIG. 4. (Color online) HHG spectrum for the combination of chirped laser and static field. The chirp parameters are $\beta=9.0$ and $t_0=\tau/8.0$.

may return back and recombine with the parent ion. During the recombination, a photon is emitted.

The returning kinetic energies of the electron in different laser fields are shown in Fig. 2. For comparison, the ionization potential is added. It is apparent that the trajectories of the electron in these field cases are quite different. Usually, there are two dominant quantum paths with different emis-

sion times contributing to each harmonic in each half optical cycle (OC) [10]: the positive slope section (short path) and negative slope section (long path) in returning kinetic-energy map. In Fig. 2(b), due to the effect of static electric field, only the short paths contribute to the harmonics above $I_p + 0.62U_p$, and the maximum returning kinetic energy (MRKE) is up to $8.0U_p$ (about 154 harmonics). That is, to say, the static electric field can eliminate some long paths of the electron. In Fig. 2(c), the long paths of the electron are not eliminated as apparently as those in Fig. 2(b), but the MRKE is up to $11.7U_p$ (about 225 harmonics) because of the chirped laser field. However, when the combination of the chirped laser and static electric field is applied, the electron returns within less than 1.5 optical cycles, and for harmonics above $I_p + 2.1U_p$, just as Fig. 2(d) displays. The MRKE is up to $27.5U_p$ (about 530 harmonics) which is much higher than the summation of that in Figs. 2(b) and 2(c). If we mark the maximum peak (cutoff energy) and the peak just below it with M and N , respectively, we can see clearly that it is the difference between the peak M and N that contributes to the continuum spectrum, as is mentioned in Ref. [8]. Just as addressed in the introduction, the continuous spectrum is beneficial to generate single attosecond pulse. This will be discussed later.

In order to explore the extremely extended cutoff, we look

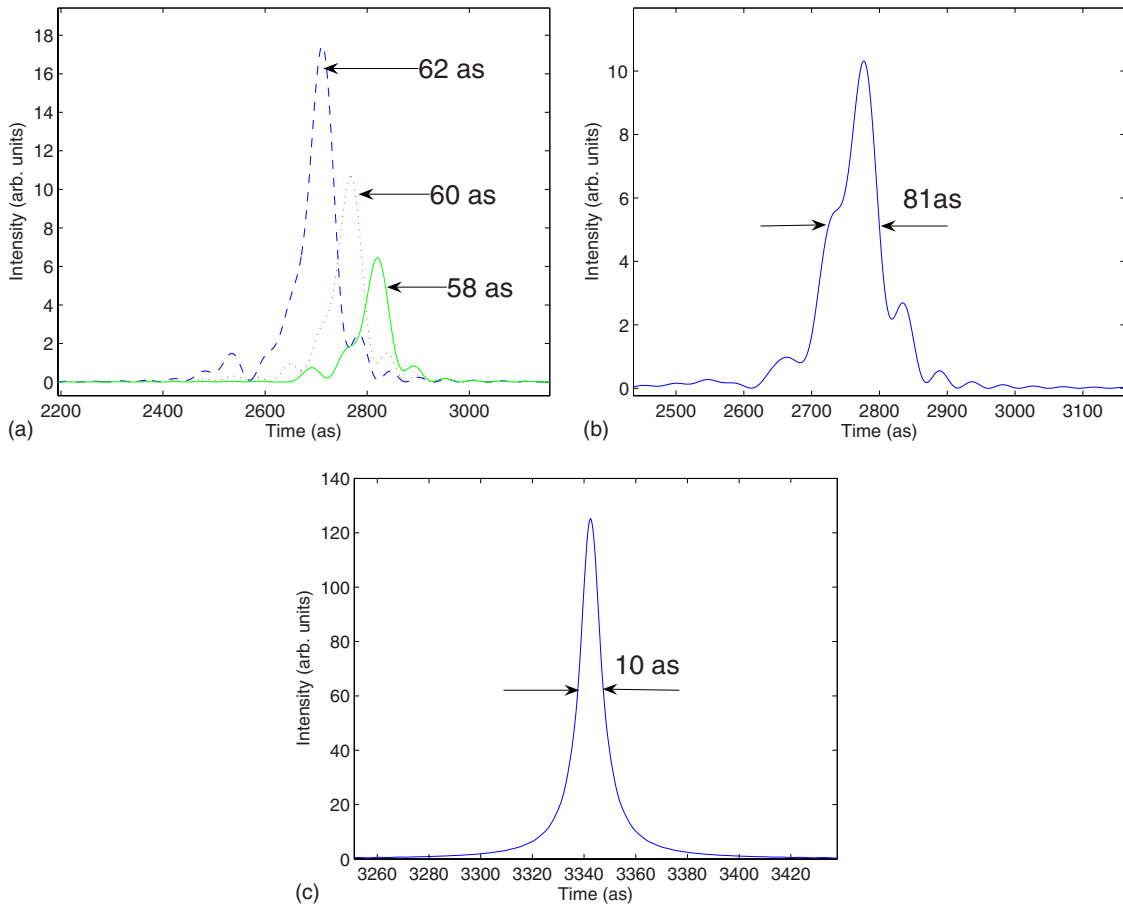


FIG. 5. (Color online) The temporal profiles of the attosecond pulses generated from the continuum spectrum from Figs. 4(a) and 4(b) without and (c) with phase compensation. The harmonics order used in (a) are 220th–270th (blue dash line), 240th–290th (red dot line), and 260th–310th (green solid line). The harmonics order used in (b) is 240th–300th. The harmonics order used in (c) is 220th–700th.

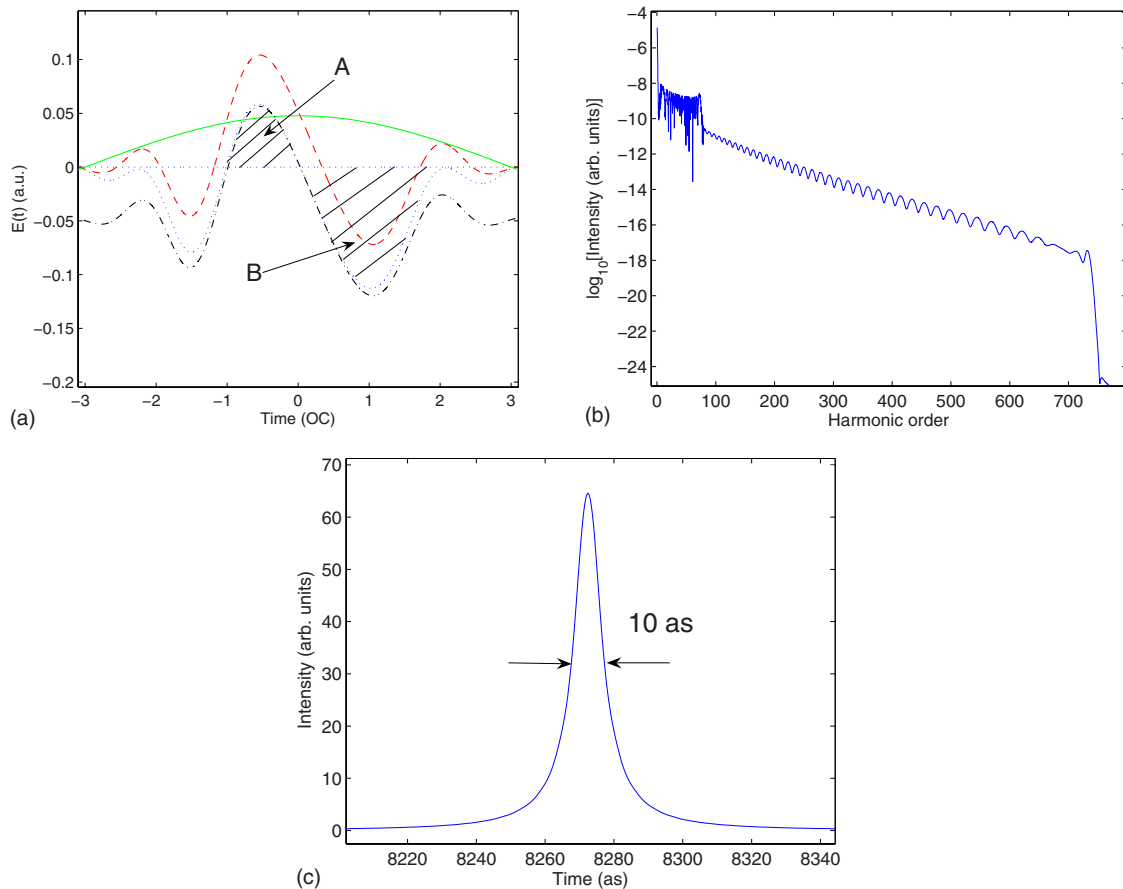


FIG. 6. (Color online) (a) Temporal profiles of the CO₂ laser field (green solid line), chirped laser field (red dashed line), combination of the CO₂ laser field and chirped laser field (blue dotted line), and combination of the chirped laser field and static electric (black dashed-dotted line); (b) the HHG spectrum in the combination of the chirped laser field and the CO₂ laser field. (c) The temporal profiles of the attosecond pulses generated from the continuum spectrum of (b) and the harmonics order used is 220th–700th.

into two processes in TSM: (i) once the electron tunnels, it accelerates in the electric field; (ii) when the electric field inverses, the electron then slows down and turn back to the parent ion. If the impulse in process (i) is weak, the kinetic energy the electron gains is small, as well as the returning kinetic energy. However, if the impulse in process (i) is strong, the impulse in process (ii) should be much stronger than the impulse in process (i), otherwise, the electron cannot return to the parent ion. So, in order to gain a large returning kinetic energy, both the impulse in process (i) and the difference between the two impulses should be large. Based on this, one can easily find the two impulses which contribute to the MRKE. These impulses are represented by the shadow areas which marked with A and B, respectively, in each field of Fig. 1. Compared with the returning energy map in Fig. 2, we find that the electron of the maximum energy just returns in area B. From Fig. 1, we can see that there is not so much difference of impulse A in the four fields. Nevertheless, due to the static electric field or the chirp, the symmetry of the field is broken. Thus, the difference of impulse B and impulse A enlarges, so the cutoff of case (b) or (c) is extended, compared with that of case (a). For the combination of the chirped laser and the static field, the symmetry is broken further, and hence there is a greater difference between impulse B and impulse A. As a result, the cutoff is extended

significantly. From the analysis above, we conclude that proper asymmetry of the field can lead to the extension of the HHG cutoff extremely.

Since the cutoff of HHG can be extremely extended in the presence of chirped laser and static electric field, it is instructive to find out how the chirp parameters impact on the HHG cutoff. The variation in the MRKE of electron with the chirp parameters β and t_0 is obtained by TSM, and the result is shown in Fig. 3. Apparently the optimal MRKE of electron is up to $42U_p$ at $\beta=9.0$ and $t_0=\tau/8.0$. The HHG spectrum for these parameters is presented in Fig. 4. One can find that the continuum spectrum is broadened to 700 order harmonics.

Now, we consider the attosecond pulse generation from HHG of Fig. 4. By adding a frequency window with a bandwidth of 50 order harmonics to the supercontinuum spectrum and making an inverse Fourier transformation, an isolated attosecond pulse is generated without any phase compensation. If we move this frequency window along harmonic order axis, the duration of the attosecond pulse changes a little, though the intensity decreases. That is to say, the pulse duration is not sensitive to the position of the frequency window. The temporal profiles of the attosecond pulses are shown in Fig. 5(a). The shortest pulse duration we show in this figure is 56 attosecond. One may think that if we enlarge the width of the frequency window, the attosecond pulse du-

ration will shorten further. Actually, due to the phase mismatch, the pulse duration lengthens but rather shortens, as shown in Fig. 5(b) [compared with the red dot line in (a)]. However, if the phase mismatch over such an ultrabroad continuum spectrum can be properly compensated for, an isolated 10 as pulse with a clean temporal profile [Fig. 5(c)] could be theoretically obtained.

Considering the practicability in experiment, we apply a CO₂ laser field instead of a static electric field which has the form of

$$E_{\text{CO}_2}(t) = 0.4F \cos(\omega_c t + \phi), \quad (4)$$

where $\omega_c = 0.0047$ a.u. and ϕ denotes frequency and absolute phase, respectively. Since the duration of the chirped laser pulse is comparable with half period of the CO₂ laser field, the absolute phase ϕ should be carefully chosen in order to make the laser pulses burst mainly in half period of the CO₂ laser field. Here we set ϕ to be zero, and therefore the CO₂ laser field does not change the sign during the whole chirped pulse [18], which just likes a “static” electric field added on the chirped pulse, as shown in Fig. 6(a). Though the CO₂ laser field does not keep constant during the whole chirped pulse, the asymmetry of the combination of the chirped laser field and CO₂ laser field (blue dotted line) has not much changes compared with the field (black dashed-dotted line) adopted in Fig. 4. That is to say, the two impulses for the processes (i) and (ii) which marked A and B

have not much difference with those of the combination of the chirped laser field and the static electric. So, as we expect, an ultrabroad continuum spectrum appears in the HHG spectrum for this combination field, as shown in Fig. 6(b). If all the phase of the continuum spectrum is properly compensated for, still an isolated 10 as pulse with clean profile can be obtained, as shown in Fig. 6(c).

In conclusion, the HHG of hydrogen atom in the combination of chirped laser field and static electric field together with that in the combination of chirped laser field and CO₂ laser field have been investigated. We demonstrated that proper asymmetry of the field lead to the significant extension of the HHG cutoff. If appropriate parameters are used, an ultrabroad continuum spectrum which covers about 700 order harmonics is obtained. By imposing a bandpass filter with bandwidth of 50 order harmonics on the continuum spectrum, a sub-100 as isolated pulse is generated without any phase compensation. If all the phase of the continuum spectrum is properly compensated for, an isolated 10 as pulse with clean profile can be obtained.

The work was supported by the National Basic Research Program of China (Grant Nos. 2006CB921104 and 60708008), the Project of Academic Leaders in Shanghai (Grant No. 07XD14030), the Key Basic Research Foundation of Shanghai (Grant No. 08JC1409702), and the Knowledge Innovation Program of the Chinese Academy of Sciences.

-
- [1] C. Winterfeldt, C. Spielmann, and G. Gerber, *Rev. Mod. Phys.* **80**, 117 (2008).
- [2] T. Pfeifer, L. Gallmann, M. J. Abel, P. M. Nagel, D. M. Neumark, and S. R. Leone, *Phys. Rev. Lett.* **97**, 163901 (2006).
- [3] Z. Zeng, Y. Cheng, Y. Fu, X. Song, R. Li, and Z. Xu, *Phys. Rev. A* **77**, 023416 (2008).
- [4] Y. Mairesse, A. de Bohan, L. J. Frasinski, H. Merdji, L. C. Dinu, P. Monchicourt, P. Breger, M. Kovacev, T. Auguste, B. Carre, H. G. Muller, P. Agostini, and P. Salieres, *Phys. Rev. Lett.* **93**, 163901 (2004).
- [5] R. Kienberger, E. Goulielmakis, M. Uiberacker, A. Baltuska, V. Yakovlev, F. Bammer, A. Scrinzi, Th. Westerwalbesloh, U. Kleineberg, U. Heinzmann, M. Drescher, and F. Krausz, *Nature (London)* **427**, 817 (2004).
- [6] Y. Mairesse, A. de Bohan, L. J. Frasinski, H. Merdji, L. C. Dinu, P. Monchicourt, P. Breger, M. Kovacev, R. Taïeb, B. Carré, H. G. Muller, P. Agostini, and P. Salières, *Science* **302**, 1540 (2003).
- [7] W. Cao, P. Lu, P. Lan, X. Wang, and Y. Li, *Phys. Rev. A* **75**, 063423 (2007).
- [8] Z. Zeng, Y. Cheng, X. Song, R. Li, and Z. Xu, *Phys. Rev. Lett.* **98**, 203901 (2007).
- [9] J. J. Carrera, X. M. Tong, and Shih-I Chu, *Phys. Rev. A* **74**, 023404 (2006).
- [10] W. Hong, P. Lu, W. Cao, P. Lan, and X. Wang, *J. Phys. B* **40**, 2321 (2007).
- [11] J. J. Carrera and Shih-I Chu, *Phys. Rev. A* **75**, 033807 (2007).
- [12] M. Protopapas, C. H. Keitel, and P. L. Knight, *Rep. Prog. Phys.* **60**, 389 (1997).
- [13] B. Borca, A. V. Flegel, M. V. Frolov, N. L. Manakov, D. B. Milosevic, and A. F. Starace, *Phys. Rev. Lett.* **85**, 732 (2000).
- [14] S. T. Cundiff and J. Ye, *Rev. Mod. Phys.* **75**, 325 (2003).
- [15] Th. Udem, R. Holzwarth, and T. W. Hänsch, *Nature (London)* **416**, 233 (2002).
- [16] K. Burnett, V. C. Reed, J. Cooper, and P. L. Knight, *Phys. Rev. A* **45**, 3347 (1992).
- [17] P. B. Corkum, *Phys. Rev. Lett.* **71**, 1994 (1993).
- [18] W. Hong, P. Lu, P. Lan, Z. Yang, Y. Li, and Q. Liao, *Phys. Rev. A* **77**, 033410 (2008).